International Journal of Bifurcation and Chaos

Critical velocity for the onset of fast Fermi acceleration

D. O. LUBCHENKO
Institute of Physics, Saratov State University, 83 Astrakhanskaya Street
Saratov, 410012, Russia
dima4398lub@mail.ru

A. V. SAVIN
Institute of Physics, Saratov State University, 83 Astrakhanskaya Street
Saratov, 410012, Russia
SavinA@info.sgu.ru

Received received

One of the well-known effects in nonlinear science is Fermi acceleration that is the unlimited growth of the velocity of a particle when it collides with oscillating walls. It is rather common for time-dependent billiard-like systems in which a particle moves inside a closed oscillating boundary and elastically collides with it. But if the oscillations are weak, more complex effects may arise in the system. Earlier one of these effects was shown for time-dependent stadium-like billiard. In the case of a weak boundary oscillation the red particle's velocity grows if its initial value is greater than a certain critical value and tends to the limit otherwise. We consider the dynamics of a particle moving between two planar and harmonically corrugated walls and colliding elastically with them. We tried to find a similar effect and revealed that the ensemble-averaged velocity grows rapidly if the initial velocity is larger than some critical value. Otherwise, the ensemble-averaged velocity grows much slower and the velocities of all particles tend to become equal. We numerically estimated the band of the oscillation amplitude in which this effect exists and illustrated the dependence of the behavior of the critical initial velocity on various parameters.

Keywords: chaotic dynamics, Fermi acceleration, time-dependent billiards

1. Introduction

The classical billiard is the dynamical system of a particle or an ensemble of non-interacting particles which move inside a closed boundary and elastically collides with it. Billiards are a popular type of conservative dynamical systems demonstrating both regular and chaotic dynamics which are well studied nowadays [Sinai, 1970], [Bunimovich, 1974], [Bunimovich, 2001], [Chernov & Markarian, 2006], [Loskutov, 2007], [Zaslasvsky, 2008].

If we let the billiard's boundary oscillate, its dynamics can change drastically because the velocity of a particle is not constant then. It is known that if the dynamics of a billiard with fixed boundaries is chaotic then in the case of the oscillation boundaries the Fermi acceleration (the unlimited growth of the ensemble average velocity) [Fermi, 1949] appears [Gelfreich & Turaev, 2008], [Dettmann, 2018]. The phenomenon of Fermi acceleration in time-dependent billiards and other systems with elastic collisions of a particle and a moving wall is studied in a number of papers both theoretically [Gelfreich & Turaev, 2008],

[Gelfreich *et al.*, 2014], [Dettmann, 2018], and numerically [Oliveira & Gonsales, 1997], [Karlis *et al.*, 2006], [Oliveira & Pöschel, 2013], [Castaldi *et al.*, 2014], [Hansen *et al.*, 2019]. The theory of Fermi acceleration in chaotic time-dependent billiards was developed in a series of papers such as [Batistic & Robnik, 2011], [Batistic, 2014-1], [Batistic, 2014-2] and it was shown that Fermi acceleration occurs if the static billiard demonstrates chaotic dynamics. Also it was shown [Lenz *et al.*, 2008] that Fermi acceleration occurs in an elliptic billiard which is regular in the static case.

However, it was shown [Livorati *et al.*, 2012] that the stickiness of the regular island boundaries, well-known for affecting the diffusion in the Hamiltonian systems [Zaslasvsky, 2008], [Manos & Robnik, 2014], [Moges *et al.*, 2022], can decrease Fermi acceleration. A similar interesting phenomenon exists in some types of billiards which have both chaotic and regular regions in the phase space. Provided we take an ensemble of particles with the equal values of the initial velocity then its average velocity grows if this velocity is larger than some value and diminishes if it is less than that value. This phenomenon is described in [Livorati *et al.*, 2012] for a stadium-type billiard with the oscillating boundaries and is called a peculiar Maxwell's Demon there.

In this paper we reveal the similar phenomenon that exists in another billiard-like system which is the corrugate waveguide [Tennyson *et al.*, 1980] with the oscillating boundary. It is well known [Lichtenberg & Lieberman, 1983] that there are areas of chaotic and regular dynamics in this system without oscillations. We study the dependence of the ensemble-averaged velocity on time for different parameters. We reveal that at some parameters the ensemble-averaged velocity grows fast if the initial velocity is larger than some values called "critical initial velocity". Otherwise, the ensemble-averaged velocity grows much more slowly and the velocity of all particles tends to become equal. We refer to the first case as fast Fermi acceleration and to the second case as slow Fermi acceleration. We numerically estimate the band of the boundary oscillation amplitude value in which this effect exists and the dependence of critical initial velocity on the parameters.

2. The model description

Consider a system in which a particle moves between two boundaries and elastically collides with them. One boundary is fixed and set by the equation:

$$y_1 = 0. \tag{1}$$

The other boundary is corrugated and can oscillate harmonically. Then its equation is:

$$y_2 = F(x,t) = b\cos kx + a\cos wt + h \tag{2}$$

In "Eq. (2)" a – the oscillation amplitude, b – the corrugation amplitude, h – the average distance between the boundaries.

The model is mechanical and it is not difficult to obtain expressions for $v_{n+1}, \alpha_{n+1}, x_{n+1}, t_{0_{n+1}}$ ("Fig. 1") in the case of the weak amplitudes of the corrugation and the oscillation. We consider the static boundary approximation, which means that we assume the position of the upper boundary fixed although its velocity changes with time. This approximation is often used [Livorati *et al.*, 2012], [Livorati *et al.*, 2014], [Palmero *et al.*, 2018] as it allows to obtain an explicit map. The discussion of the possible effect of this approximation is given in the conclusion. So, these expressions form the 4D map:

$$\begin{cases} v_{n+1} = \sqrt{v_{n+1_x}^2 + v_{n+1_y}^2}; \\ \alpha_{n+1} = \arctan\frac{v_{n+1_x}}{v_{n+1_y}}; \\ x_{n+1} = x_n + 2h\frac{v_{n+1_x}}{v_{n+1_y}}; \\ t_{0_{n+1}} = t_{0_n} + \frac{2h}{v_{n+1_y}}. \end{cases} \tag{3}$$

In "Eq. (3)": $v_{n+1_x} = v_n\sin(\alpha_n + 2\gamma) - 2\gamma u$, $v_{n+1_y} = v_n\cos(\alpha_n + 2\gamma) - 2u$, $u = -aw\sin wt_{0_n}$,

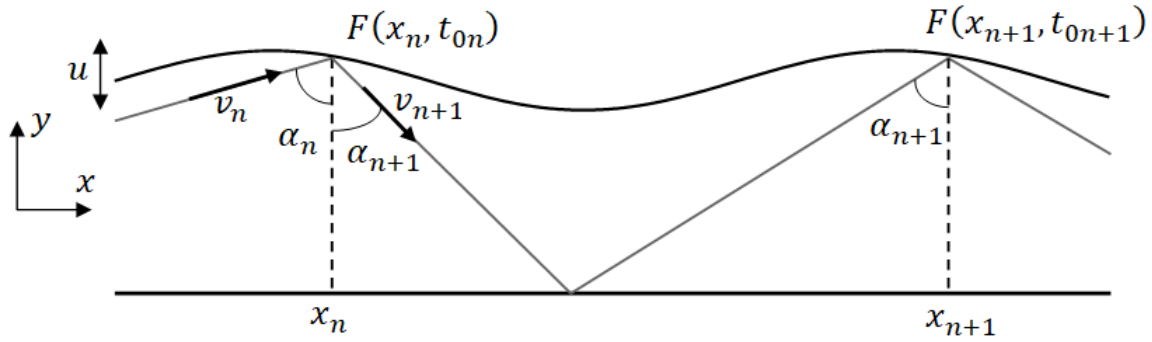

Fig. 1. Illustration of the particle movement between two boundaries. x_n – the coordinate of the n-th collision with the upper boundary; α_n – the angle between the normal to the bottom boundary and the velocity vector at the moment of the n-th collision v_n; v_n – the particle velocity at the moment of the n-th collision with the upper boundary; t_{0_n} – the elapsed time from the moment the particle begins to move until the moment of the n-th collision with the upper boundary.

$\gamma = -kb \sin kx_n$. The number of the parameters can be reduced via the following replacement:

$$\begin{cases} \phi_n = kx_n; \\ \psi = wt_{0_n}; \\ \Omega = \frac{v_{nx,y}}{2hw}; \\ A = 2hk \\ B = \frac{a}{h} \\ C = bk \end{cases} \tag{4}$$

It results in the 4D map with four parameters:

$$\begin{cases} \Omega_{n+1} = \sqrt{\Omega_{n+1_x}^2 + \Omega_{n+1_y}^2} \\ \alpha_{n+1} = \arctan\left[\frac{\Omega_{n+1_x}}{\Omega_{n+1_y}}\right] \\ \phi_{n+1} = \phi_n + A\frac{\Omega_{n+1_x}}{\Omega_{n+1_y}} \\ \psi_{n+1} = \psi_n + \frac{1}{\Omega_{n+1_y}} \end{cases} \tag{5}$$

In "Eq. (5)": $\Omega_{n+1_x} = \Omega_n \sin(\alpha_n + 2\gamma) - 2\gamma u$, $\Omega_{n+1_y} = \Omega_n \cos(\alpha_n + 2\gamma) - 2u$, $\gamma = -C \sin \phi_n, u = -B \sin \psi_n, \Omega_n$ – the dimensionless velocity, ϕ_n – the dimensionless coordinate, ψ_n – the dimensionless time, A — the dimensionless average distance between the boundaries, B — the dimensionless oscillation amplitude, C — the dimensionless corrugation amplitude.

Consider a degenerate situation when the top boundary is fixed ($B = 0$). In this case $u = 0$ and the velocity does not change over time. Then system "Eq. (5)" is reduced to the two-dimensional map:

$$\begin{cases} \alpha_{n+1} = \alpha_n - 2C \sin \phi_n \\ \phi_{n+1} = \phi_n + A \tan \alpha_{n+1} \end{cases} \tag{6}$$

The resulting system is the restricted case of well-known Tennyson-Lieberman-Lichtenberg map [Tennyson *et al.*, 1980], [Lichtenberg & Lieberman, 1983]. The structure of the phase space is typical for non-integrable two-dimensional Hamiltonian systems. They have the regular trajectories that are quasi-periodic (KAM) tori and the chaotic ones that are destructed tori. The structure of the system's phase space in a small range of the parameters is to be considered. The parameters' variation is small because we are interested in the phenomena which occur in the case of the weak nonlinearity. It must be kept in mind that phase space structure can change significantly if a larger range of the parameters' change is taken. In "Fig. 2" the way the phase space structure is transformed depending on the boundary corrugation (parameter C) is shown. In fact, parameter C is the nonlinearity parameter because if it is increased, the

number of the destroyed tori grows. In "Fig. 3" the way the phase space structure is transformed depending on the distance between the boundaries (parameter A) is shown. It can be seen that if this parameter is changed, the phase space does not vary topologically but the size of chaotic region and the stability islands changes. We choose the parameters $A = 2$ and $C = 0.05$ which correspond to the case of the weak corrugation ($C \ll A$) for futher simulation.

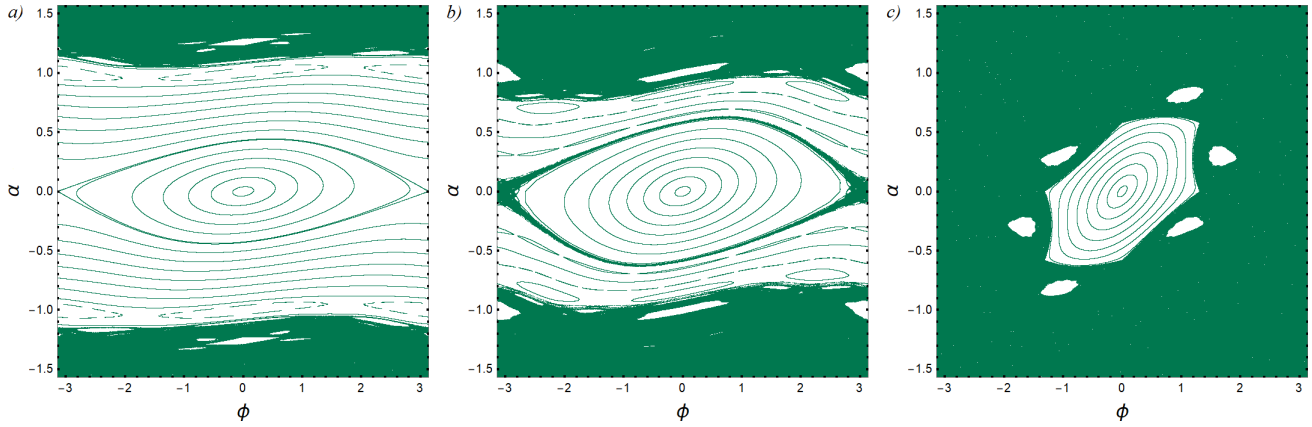

Fig. 2. Phase portrait of the system "Eq. (6)" with the parameters: $A = 2$ and $C = 0.05$ (a); $C = 0.1$ (b); $C = 0.3$ (c).

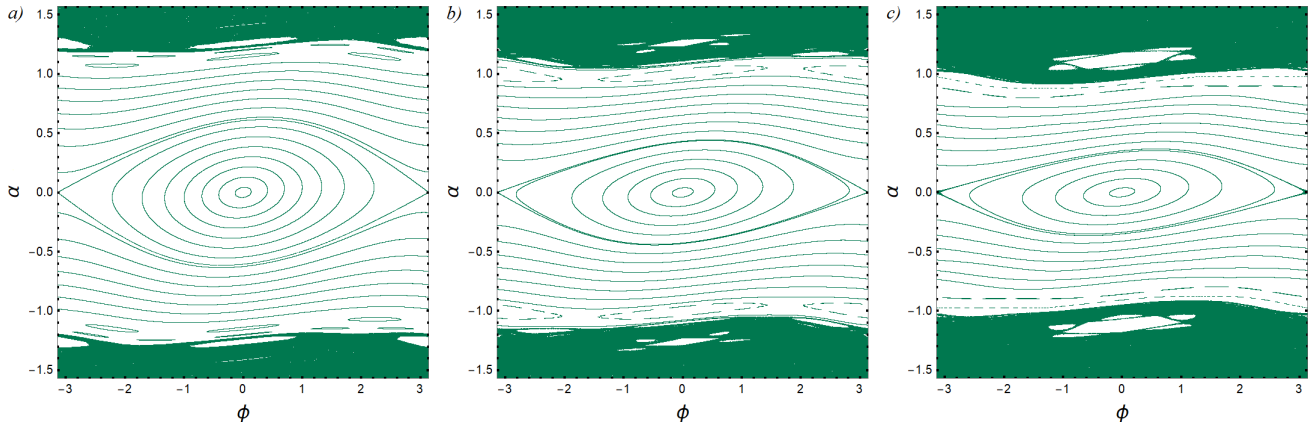

Fig. 3. Phase portrait of the system "Eq. (6)" with the parameters: $C = 0.05$ and $A = 1$ (a); $A = 2$ (b); $A = 3$ (c);

3. The dynamics of ensemble-averaged velocity

Let us consider the system which is given by "Eq. (5)". The evolution of the projection of the trajectories of the ensemble of initial conditions on (ϕ, α)-plane is shown in "Fig. 4". We use the ensemble of 4410 initial conditions with the same initial velocity (Ω_0) and different initial values of other variables that were selected on the cubic lattice in the chaotic region ($\phi_0 \in [0; 3]$, $\alpha_0 \in [0.35\pi; 0.4\pi]$), $\psi_0 \in [0; 3]$). It is known that if a trajectory is chaotic then its largest Lyapunov exponent (LLE) is larger than zero. We calculate LLE for each initial condition of the ensemble for the situation when $B = 0$, they are positive in most cases and their average value $\bar{\Lambda} = 0.98$. As we can see in "Fig. 4a", in this case the initial conditions are both in the chaotic and in the regular regions. For $B = 0.01$ LLE is positive for all initial conditions, its average value $\bar{\Lambda} = 1.23$ and "Fig. 4b" shows that the chaotic region becomes larger than at $B = 0$. For $B = 0.03$ ("Fig. 4c"), we can still see stability regions, however, the chaotic trajectories penetrate into

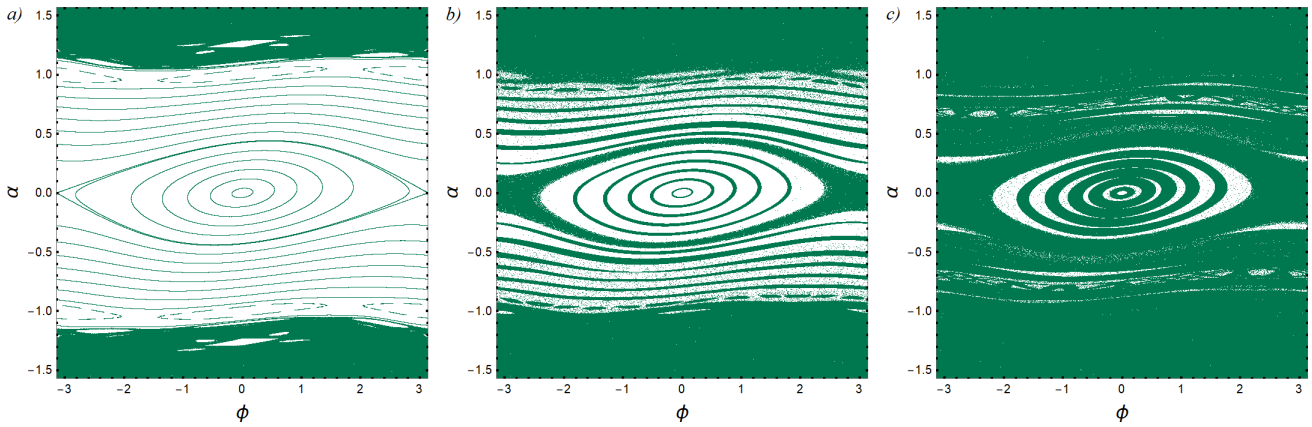

Fig. 4. Phase portrait of the system "Eq. (5)" with the parameters: $A = 2, C = 0.05$ and $B = 0$ (a); $B = 0.01$ (b); $B = 0.03$ (c).

them due to the Arnold's diffusion [Arnol'd, 1964]. We did not consider the projection of the phase space on (ψ, Ω) because individual structures cannot be seen on it.

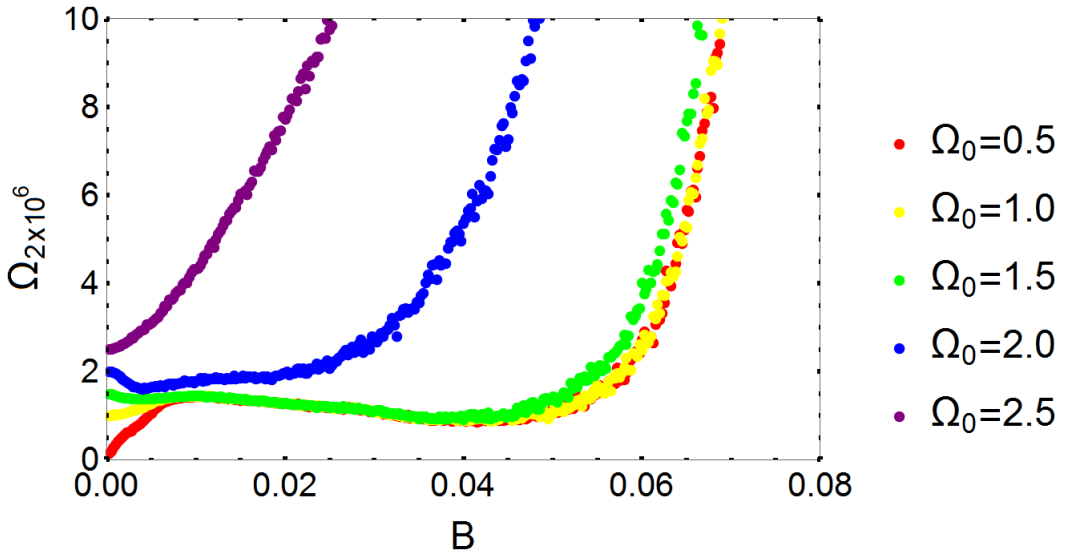

Fig. 5. Dependence of the ensemble-averaged velocity after 2.000.000 iterations (Ω_{2x10^6}) of "Eq. (5)" with the parameters $A = 2, C = 0.05$ on the oscillation amplitude. The color of a curve shows the initial velocity Ω_0, whose values are in the figure.

Then we try to find the region where Fermi acceleration can be observed starting from a certain value of the initial velocity. To achieve this we build the plots of the ensemble-averaged velocity after 2.000.000 iterations (Ω_{2x10^6}) of "Eq. (5)" on the oscillation amplitude B at different initial velocities ("Fig. 5"). It can be seen that three curves ($\Omega_0 = 0.1, \Omega_0 = 1.0, \Omega_0 = 1.5$) are very close for B between 0.01 and 0.04. They begin to increase rapidly starting from a certain value of the amplitude whereas other curves are always located above them. It can be assumed that there is a region of the oscillation amplitude in which particles whose initial velocity is below a certain value begin to move with a common velocity. If the initial velocity of the particles is higher than this value, they accelerate. Furthermore, from this overlapping part we can estimate the domain of the amplitude of oscillations where the movement with a common velocity can be observed.

Now we consider the different points of the proposed domain. The plot of the average velocity on the number of iterations of the system "Eq. (5)" is shown in "Fig. 6". To make sure that there are enough initial

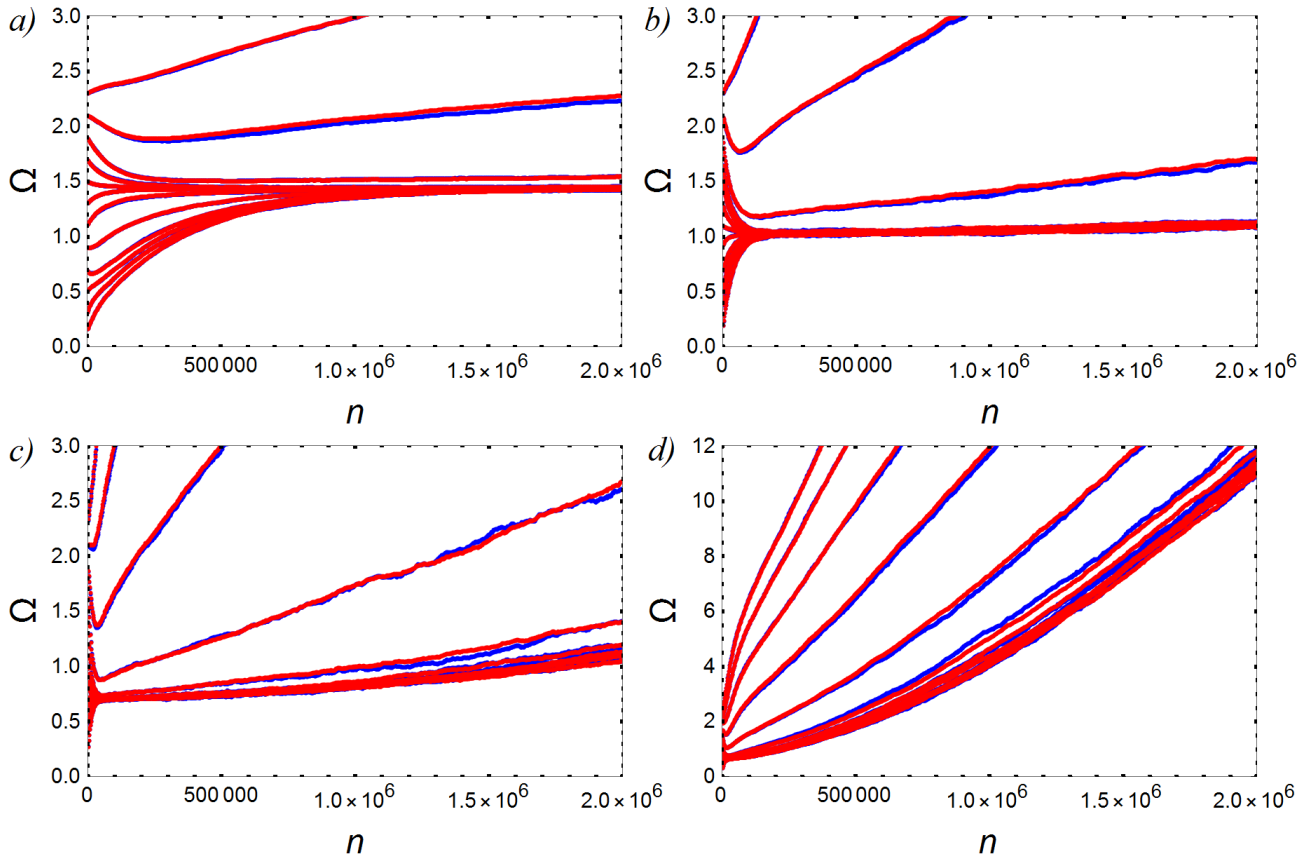

Fig. 6. Dependence of the ensemble-averaged velocity on the number of the iterations of the system "Eq. (5)" with different initial ϕ_0, ψ_0, α_0 selected on the cubic lattice in the chaotic region: $A = 2, C = 0.05$ and $B = 0.01$ (a); $B = 0.03$ (b); $B = 0.05$ (c); $B = 0.07$ (d). The initial velocity Ω_0 is taken in the range from 0.5 to 2.3 in increments of 0.2. The color of the curve depends on the number of the initial conditions: blue – 4410, red – 10140.

conditions (4410) to draw some conclusions we increase the number of the initial conditions to 10140. In Fig. 6 the data for 10140 initial conditions (red curves) coincide with the data for 4410 ones (blue curves).

For $B = 0.01$ ("Fig. 6a") and $B = 0.03$ ("Fig. 6b") it can be observed that the graphs with the initial velocity below the certain critical value tend to the common velocity. The trajectories with initial velocity larger than the critical value grow with the number of iterations. In fact, the common velocity is not a constant; it slowly grows with the number of iterations. The differences between these graphs are in the values of the common and critical velocities and also in the velocity growth rate with the same initial velocity. At $B = 0.05$ ("Fig. 6c") and $B = 0.07$ ("Fig. 6d") a similar situation is observed. However, the common velocity perceptibly increases with the number of iterations. We can state the following, more important, conclusions by analyzing these plots. First, the data for 10140 initial conditions well matches the data for a fewer number of the initial conditions in the ensemble and the number of 4410 initial conditions is sufficient for the statistical analysis of the system. Second, the critical value of the initial velocity appears in the system for the certain values of the parameters and trajectories which have the initial velocity below this value tend to the same common velocity. Third, there is the domain of parameter B where the common velocity slowly increases with time. It can be assumed that in this situation trajectories that move with a common velocity have slow Fermi acceleration and trajectories which have the initial velocity above the critical one have fast Fermi acceleration.

In order to see the differences in particle velocity growth at different initial velocities, we plot the difference $(\Delta\Omega)$ of the ensemble-averaged velocities after 3.000.000 iterations and 2.000.000 iterations (actually, it is averaged acceleration) depending on the initial velocity at different parameter B ("Fig. 7"). The ensemble consists of 4410 initial conditions as described above. In "Fig. 7a" this dependence for

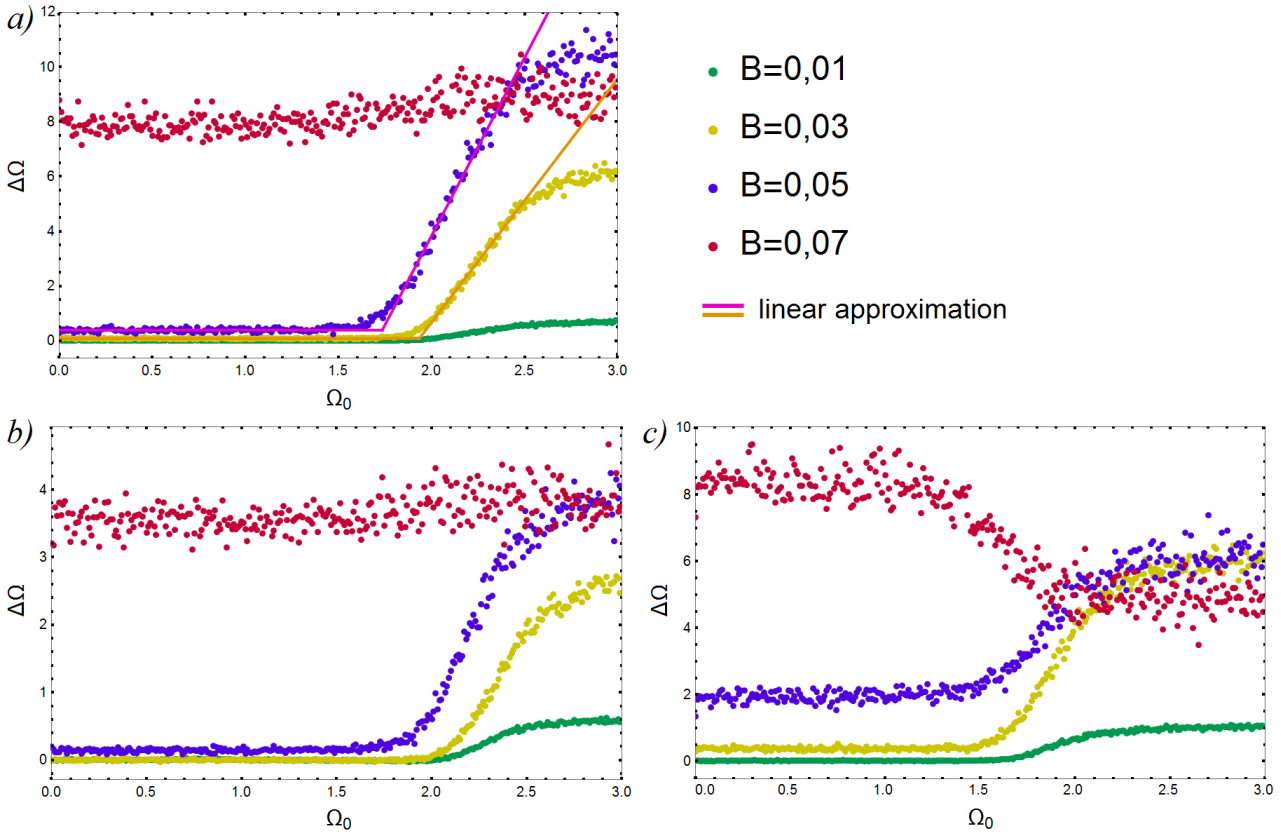

Fig. 7. Dependence of the difference between the ensemble-averaged velocity after 3.000.000 iterations and 2.000.000 iterations ($\Delta\Omega$) of the system "Eq. (5)" (in fact, it is acceleration) on the initial velocity for different values of the oscillation amplitude B which are shown in the figure. Parameters: $A = 2, C = 0.05$ (a); $A = 3, C = 0.05$ (b); $A = 2, C = 0.06$ (c).

parameters $A = 2, C = 0.05$ with different B is shown. The values of parameter B are displayed in the figure. It can be seen that for $B = 0.01, 0.03, 0.05$ the curves have a horizontal segment that is close to zero followed by the increasing segment. The $\Delta\Omega$ remains nearly constant for large Ω_0. For $B = 0.07$ it is difficult to divide the curve into some stages due to the large spread of the acceleration values. We made a linear approximations of the horizontal and the increasing parts of the curves (see Fig.7a for example), and estimate the critical velocity as the intersection point of these lines. In "Fig. 7b" a graph for $A = 3, C = 0.05$ is shown. There are no qualitative distinctions from "Fig. 7a", however, the absolute values of the accelerations are different. At parameters $A = 2, C = 0.06$ ("Fig. 7c") the curve for $B = 0.07$ has an area where the acceleration decreases with the increase of the initial velocity.

Now let us calculate the range of the parameter B in which we can observe slow and fast Fermi acceleration. We plot the dependence of $\Delta\Omega$ on the horizontal segment (for example, its value at $\Omega_0 = 1.0$) on the amplitude of the boundary oscillations ("Fig. 8") for that. The curves are plotted for different values of the parameters A and C. For B less than 0.07 these plots are well approximated by an expression $\Delta\Omega = ae^{cB} + b$, where a, b, c are constants specific for each curve. We use this fact to estimate the "critical" value B_{cr} that is the value at which $\Delta\Omega$ becomes e times larger than its value at $B = 0.01$. We assume that there is no separation into fast and slow Fermi acceleration when the amplitude of the boundary oscillations is greater than B_{cr}. The results of the calculation B_{cr} by this method are shown in "Table 1". It can be seen that the value of B_{cr} decreases with the increase of the parameters A and C.

Another issue worth considering is the dependence of the critical velocity on the oscillation amplitude. "Fig. 9a" shows it for different values of the parameters A and C. The curves seem to be rather similar. The parabolic approximations of the data are plotted in "Fig. 9b". It can be seen that critical velocity does not exceed 2.0 for all curves at $B \in (0; B_{cr})$ (B_{cr} is different for each curve). Somewhere with $B \approx 0.024$, the values of the critical velocities have a minimum spread of values for different parameters. Before $B \approx 0.05$,

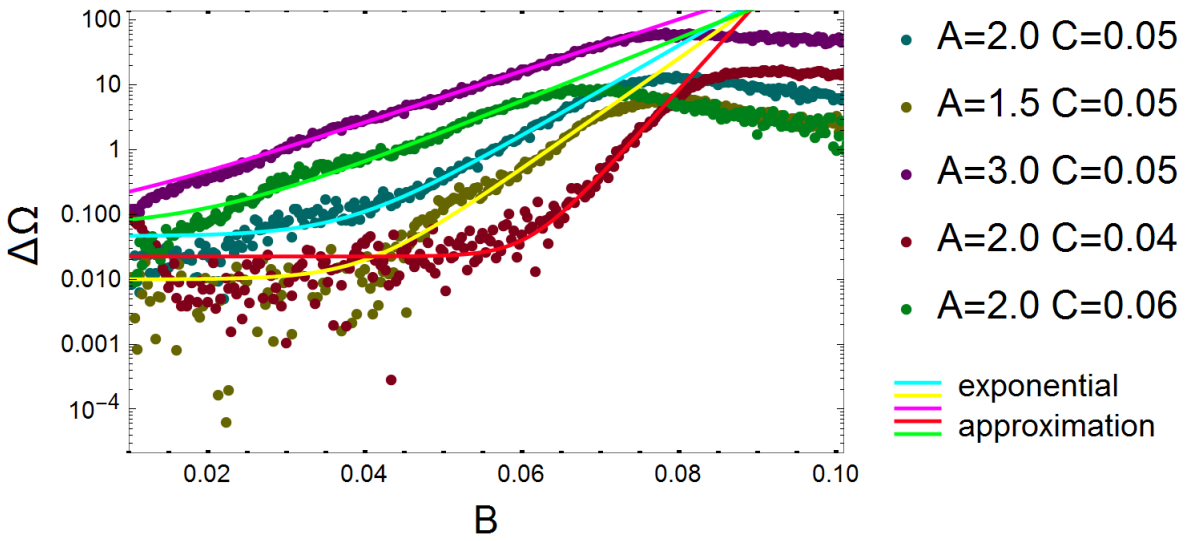

Fig. 8. Dependence of the value of the horizontal section on parameter B of the system "Eq. (5)" on a logarithmic scale for different parameters A and C whose values are shown in the figure.

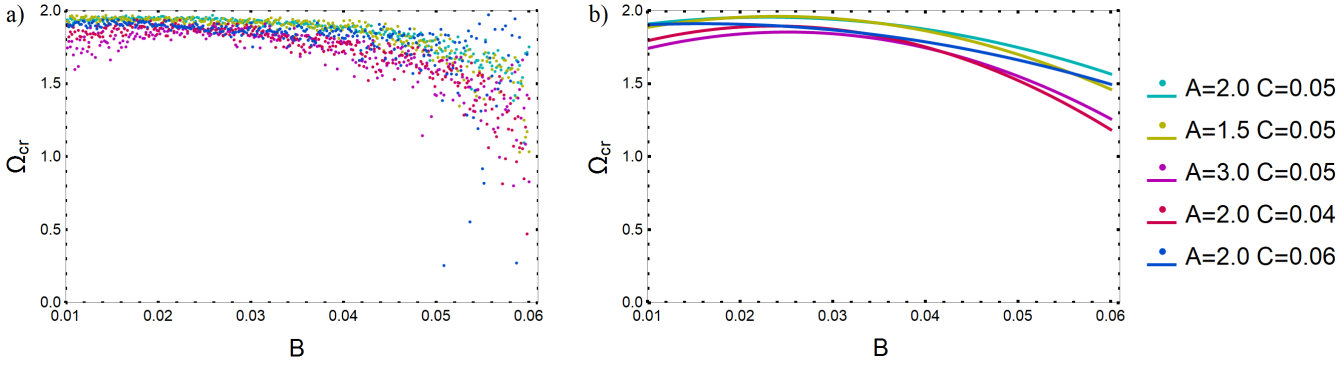

Fig. 9. Dependence of the critical velocity on the boundaries oscillations amplitude of the system "Eq. (5)" for different parameters A and C whose values are shown in the figure. (a) The numerical data; (b) the approximations.

Table 1. Dependence of B_{cr} on different parameters A and C.

A	C	B_{cr}
2.0	0.05	0.041
1.5	0.05	0.043
3.0	0.05	0.023
2.0	0.04	0.063
2.0	0.06	0.028

the values of the critical velocities are greater than 1.5. At $B \approx 0.06$, some curves have a large calculation error due to the fact that the linear growth area becomes smaller ("Fig. 7"), and the curve's spread becomes larger. Therefore, it is incorrect to determine the critical velocity for curves which have $B > B_{cr}$.

4. Conclusion

The research shows numerically that the system of Tennison-Liechtenberg-Lieberman with weak oscil-

lating boundary demonstrates the "classical" or fast Fermi acceleration only if the initial velocity is higher than some critical value. Otherwise, the velocity for different trajectories tends to the common value which increases gradually with time. We refer to this situation as slow Fermi acceleration. This effect is similar but not identical to the the Maxwell's Demon in billiard [Livorati *et al.*, 2012]. We assume that this effect may occur because both focusing and scattering elements of the boundary exist in the system unlike the stadium-like billiard. The transition from slow to fast Fermi acceleration is smooth: the acceleration exponentially depends on oscillation amplitude, so the critical velocity is well determined only for rather small amplitude (up to $B \approx 0.05$). It should be marked that the velocity of different trajectories with initial velocity less than the critical one tends to the same value. This effect seems to be similar to the effect in the Ulam system [Ulam, 1961]. It is known [Zaslavsky & Chirikov, 1964] that in the Ulam system the invariant KAM-tori exist at the large values of velocity and prevent the acceleration. We suppose that in the system the common velocity increases gradually due to the Arnold diffusion. Also it is interesting that the acceleration can diminish (for example, "Fig. 7c") and we think this effect deserves further research.

Another question to be discussed is whether the approximations made in the considered system affect the studied phenomenon significantly. We assume that it is unlikely due to the following reason. The error of the static wall approximation is negligible if the wall does not move significantly while the particle travels between the collisions. In our case the approximate value of the dimensionless critical velocity is 2, so the correction is to be of the same order of magnitude as $\frac{B}{4}$ which is less than 1 percent. We assume that it does not affect the studied dynamics significantly. Also, we did not take into account the cases of repeated collisions inside the focusing part of the boundary in contrast to the work of Livorati and Loskutov [Livorati *et al.*, 2012]. It does not affect the discussed phenomenon because the angle α should be small for the repeated collisions to take place but in the chaotic area α is close to $\frac{\pi}{2}$.

References

Arnol'd, V. I. [1964] "Instability of dynamical systems with many degrees of freedom," *Dokl. Akad. Nauk SSSR* **156**, 9—12.

Batistic, B. [2014] "Fermi acceleration in chaotic shape-preserving billiards," *Phys. Rev. E* **89**, 022912.

Batistic, B. [2014] "Exponential Fermi acceleration in general time-dependent billiards," *Phys. Rev. E* **90**, 032909.

Batistic, B. & Robnik, M. [2011] "Fermi acceleration in time-dependent billiards: theory of the velocity diffusion in conformally breathing fully chaotic billiards," *J. Phys. A: Math. Theor.* **44**, 365101.

Bunimovich, L. A. [2001] "Mushrooms and other billiards with divided phase space," *Chaos* **11**, 802.

Bunimovich, L. A. [1974] "On ergodic properties of certain billiards," *Funktsional. Anal. i Prilozhen.* **8**, 73–74.

Castaldi, B., Egydio de Carvalho, R., Vieira Abud, C. & Mijolaro A. P. [1989] "Tunable Fermi acceleration in a nondissipative driven magnetic billiard," *Phys. Rev. E* **89**, 012916.

Chernov, N. & Markarian, R. [2006] *Chaotic Billiards*, *Mathematical Surveys and Monographs* **127** (American Mathematical Society, USA).

Dettmann, C. P., Fain, V. & Turaev, D. [2018] "Splitting of separatrices, scattering maps, and energy growth for a billiard inside a time-dependent symmetric domain close to an ellipse," *Nonlinearity* **31**, 667-–700.

Fermi, E. [1949] "On the origin of the cosmic radiation," *Phys. Rev.* **75**, 1169.

Gelfreich, V., Rom-Kedar, V. & D. Turaev [2014] "Oscillating mushrooms: adiabatic theory for a non-ergodic system," *J. Phys. A: Math. Theor.* **47**, 395101.

Gelfreich, V. & Turaev, D. [2008] "Unbounded energy growth in Hamiltonian systems with a slowly varying parameter," *Commun. Math. Phys.* **283**, 769.

Hansen, M., Ciro, D., Caldas, I. L. & Leonel, E. D. [2019] "Dynamical thermalization in time-dependent billiards," *Chaos* **29**, 103122.

Karlis, A. K., Papachristou, P. K., Diakonos, F. K., Constantoudis, V. & Schmelcher, P. [2006] "Hyperacceleration in a stochastic Fermi-Ulam model," *Phys. Rev. Lett.* **97**, 194102.

Lenz, F., Diakonos, F. K. & Schmelcher, P. [2008] "Tunable Fermi acceleration in the driven elliptical

billiard," *Phys. Rev. Lett.* **100**, 014103.
Lichtenberg, A. J. & Lieberman, M. A. [1983], *Regular and Chaotic Dynamics*, 1st Ed., *Applied Mathematical Sciences* **38** (Springer-Verlag, New York).
Livorati, A. L. P., Palmero, M. S., Dettmann, C. P., Caldas, I. L. & Leonel, E. D. [2014] "Separation of particles leading either to decay or unlimited growth of energy in a driven stadium-like billiard," *J. Phys. A: Math. Theor.* **47**, 365101.
Livorati, A. L. P., Loskutov, A. & Leonel, E. D. [2012] "A peculiar Maxwell's Demon observed in a time-dependent stadium-like billiard," *Phys. A* **391**, 4756—4762.
Livorati, A. L. P., Kroetz, T., Dettmann, C.P., Caldas, I. L., Leonel, E. D. [2008] "Stickiness in a bouncer model: A slowing mechanism for Fermi acceleration," *Phys. Rev. E* **86**, 036203.
Loskutov, A. [2007] "Dynamical chaos: systems of classical mechanics," *Phys.-Usp.* **50**, 939–964.
Manos, T. & Robnik, M. [2014] "Survey on the role of accelerator modes for anomalous diffusion: The case of the standard map," *Phys. Rev. E* **89**, 022905.
Moges, H. T., Manos, T. & Skokos, C. [2022] "Anomalous diffusion in single and coupled standard maps with extensive chaotic phase spaces," *Phys. D* **431**, 133120.
Oliveira, D. F. M. & Pöschel, T. [2013] "Competition between unlimited and limited energy growth in a two-dimensional time-dependent billiard," *Phys. Lett. A* **377**, 2052–2057.
de Oliveira, C. R. & Gonçalves, P. S. [1997] "Bifurcations and chaos for the quasiperiodic bouncing ball," *Phys. Rev. E* **56**, 4868.
Palmero, M. S., Livorati, A. P., Caldas, I. L. & Leonel, E. D. [2018] "Ensemble separation and stickiness influence in a driven stadium-like billiard: A Lyapunov exponents analysis," *Commun. Nonlinear Sci. Numer. Simulat.* **65**, 248–259.
Sinai, Ya. G. [1970] "Dynamical systems with elastic reflections," *Russ. Math. Surv.* **25**, 137.
Tennyson, J. L., Lieberman, M. A., & Lichtenberg, A. J. [1980] "Diffusion in near-integrable hamiltonian systems with three degrees of freedom," *AIP Conf. Proc.* **57**, 272.
Ulam, S. M.[1961] "On some statistical properties of dynamical systems," *Berkeley Sympos. Math. Stat. Prob.* **4.3**, 315.
Zaslasvsky, G. M. [2008] *Hamiltonian Chaos and Fractional Dynamics*, 1st Ed. (Oxford University Press, Oxford).
Zaslavsky, G. M. & Chirikov, B. V. [1964] "Fermi acceleration mechanism in the one-dimensional case" *Dokl. Akad. Nauk SSSR* **159**, 306—309.

Acknowledgments

D.L. thanks the Ministry of Science and Higher Education of Russia for financial support (program for employment of 2020 graduates for scientific positions in universities and research institutions)